Energy Conversion and Management 199 (2019) 112047

Contents lists available at ScienceDirect

Energy Conversion and Management

journal homepage: www.elsevier.com/locate/enconman

# Thermodynamic analysis of compressed air energy storage (CAES) hybridized with a multi-effect desalination (MED) system

Amirreza Razmi[a,b], M. Soltani[a,c,d,e,*], Mohammad Tayefeh[a], M. Torabi[b], M.B. Dusseault[c,d]

[a] Department of Mechanical Engineering, K.N. Toosi University of Technology, Tehran, Iran
[b] Renewable Energy Department, Niroo Research Institute (NRI), Tehran, Iran
[c] Waterloo Institute for Sustainable Energy (WISE), University of Waterloo, Waterloo, Ontario, Canada
[d] Department of Earth & Environmental Sciences, University of Waterloo, Waterloo, Ontario, Canada
[e] Advanced Energy Initiative Center, K.N. Toosi University of Technology, Tehran, Iran

ARTICLE INFO

*Keywords:*
Multi-effect desalination
High temperature thermal energy storage
Compressed air energy storage
MED
CAES
Thermodynamics

ABSTRACT

Compressed air energy storage is one of two existing grid-scale energy storage technologies. It can be efficiently used in dry and warm climates, where providing both electricity and potable water is indispensable. A novel integration of compressed air energy storage and multi-effect desalination system is proposed to reduce energy dissipation, exergy destruction and provide power and potable water. Compression heat in the charging period is conveyed to the desalination unit; during discharging, the remaining energy in the turbine exhaust is reassigned to the desalination unit after passing through the recuperator. Round trip efficiency is thereby improved while providing peaking power and pure water. Besides, the effect of the maximum to minimum pressure ratio of the compressed air vessel on efficiency and the operational period of the system is studied for a particular set of circumstances. Results indicate that 38 kg/s potable water is produced during charging, whereas 80 MW electricity and 62.5 kg/s distilled water are concurrently generated during peak demand periods. As a result, 69.95% round trip efficiency and 9.47 performance ratio are obtained for the proposed hybrid system.

## 1. Introduction

Energy and water management are crucial societal concerns resulting from population growth in recent decades [1]. Globally, more than a billion people suffer from unreliable power and water [2]. Predictions suggest increases of 33% and 55% in power and water demands respectively from 2014 to 2050 [3]. Currently, fossil fuels provide 86% of the total global energy generation, with predicted harsh consequences of global warming and other impacts (particulates, Ozone depletion, etc.) [4]. Climate change combined with water and energy scarcity have great potential for social disruptions in the future. To manage these concerns, various actions such as renewable energy development, desalination system deployment, increased energy efficiency, and fleet electrification must take place. Provisions for such actions are explicitly recognized in environmental protocols promulgated in Montréal, Kyoto, and Paris in recent years [5].

Renewable energy sources displacing fossil fuel use can reduce the rate of global warming and ozone depletion from greenhouse gas effects [6]. However, their irregular and variable power generation is a major drawback to their use in grids that need peak shaving, load leveling, and responses to sharp demand changes [7]. Large-scale energy storage systems (ESS) appear indispensable to accommodate more and more renewable energy sources [8]. ESS improves the economic feasibility of renewable energy provision [9], so developing ESS technologies can reduce the environmental effects of fossil fuels, improve grid and energy efficiency, and provide the potential for the adoption of more renewable energy [10].

Compressed air energy storage (CAES) is one of two available grid-scale energy storage systems [11]. CAES is superior to pumped hydro energy storage (PHES) because of its relatively longer life time, much lower environmental impact, shorter construction time, higher reliability and lower installation costs [12]. PHES sites are generally geographically constrained, as they must be appropriate for the construction of dams to pool large volumes of water [13]. A lower round-trip efficiency of CAES (50–70%) in comparison to PHES (85–90%) is considered a drawback; this arises because of significant heat losses in compressors and natural gas turbine exhaust [14]. Thus, various types of auxiliary systems such as heat storage, organic rankine cycle (ORC)

* Corresponding author at: Department of Mechanical Engineering, K.N. Toosi University of Technology, Tehran, Iran; Department of Earth & Environmental Sciences, University of Waterloo, Waterloo, Ontario, Canada.
*E-mail addresses:* amirreza_razmi@yahoo.com (A. Razmi), msoltani@uwaterloo.ca (M. Soltani).

https://doi.org/10.1016/j.enconman.2019.112047
Received 4 June 2019; Received in revised form 4 September 2019; Accepted 7 September 2019
Available online 19 September 2019

**Nomenclature**

| | |
|---|---|
| $C_p$ | Specific heat of air at constant pressure [kJ/kg.K] |
| $C_{r,com}$ | Compression ratio of the air compressors |
| $C_v$ | Specific heat of air at constant volume [kJ/kg.K] |
| $E$ | Effectiveness [%] |
| $h_x$ | Specific enthalpy at point x [kJ/kg] |
| $K$ | Ratio of specific heats ($C_P/C_V$) |
| $M$ | Mass size of HTES [ton] |
| $\dot{m}_{in}$ | Inlet mass flow rate of the CAES [kg/s] |
| $\dot{m}_{out}$ | Outlet mass flow rate of the CAES [kg/s] |
| $\dot{m}_x$ | Mass flow rate at point x [kg/s] |
| $P_x$ | Pressure at point x [bar] |
| $P_r$ | Maximum to minimum pressure ratio of *CAES* |
| $PR$ | Performance ratio |
| $\dot{Q}_x$ | Heat transfer rate at point x [kW] |
| $R$ | Universal specific gas constant of air [kJ/kg.K] |
| $RTE$ | Round trip efficiency [%] |
| $s_x$ | Specific entropy at point x [kJ/kg.K] |
| $T_x$ | Temperature at point x [K] |
| $t$ | Time [hr] |
| $V_{CAES}$ | Volume of the CAES [$m^3$] |
| $\dot{W}_x$ | Power consumption at point x [kW] |
| $X$ | Salinity [%] |
| $\eta_x$ | Isentropic efficiency at point $x$ |
| $\rho$ | Density [$kg/m^3$] |

*Subscripts*

| | |
|---|---|
| 0 | Dead condition |
| *Aftc* | Aftercooler |
| *BR* | Brine |
| *CAES* | Compressed air energy storage |
| *c* | Cooling |
| *ch* | Charging |
| *CM* | Condensate mixer |
| *com* | Compression train |
| $com_1$ | First stage air compressor |
| $com_2$ | Second stage air compressor |
| *CO* | Condensate |
| *Con* | Steam condenser |
| *D* | Demister |
| *Des* | Desalination |
| *dis* | Distilled water |
| *diss* | Dissipation heat |
| *dsch* | Discharging |
| *E* | Evaporator |
| *F* | Flash |
| *HTES* | High temperature thermal energy storage |
| *Intc* | Intercooler |
| *M* | Steam mixer |
| *MED* | Multi effect desalination |
| *op* | Operating temperature |
| *P* | Preheater |
| *Rec* | Recuperator |
| *Reg* | Pressure regulating valve |
| *s* | Isentropic |
| *ST* | Steam |
| *SW* | Sea water |
| *SWR* | Sea water rejected |
| *Tur* | Turbine |

engines, ejectors, refrigeration and Kalina cycles may be combined with CAES to enhance its performance. For example, Sadreddini et al. [15] investigated a novel cogeneration system including CAES, ORC and ejector subsystems, able to provide power, cooling and heating capacities, simultaneously. Zhao et al. [16] coupled CAES with the Kalina cycle, recovering energy from the recuperator by the Kalina cycle to achieve higher efficiencies. Jannelli et al. [17] introduced a hybrid system containing photovoltaic power, CAES and thermal energy storage (TES) systems for a storage system efficiency (SSE) of 57%. A novel hybridization of CAES with an absorption-recompression refrigeration cycle was introduced by Razmi et al. [8]. They used high temperature thermal energy storage (HTES) concept instead of the conventional combustion chambers in CAES unit and analyzed their proposed hybrid system from the energy, exergy and economic points of view, concluding that their environmentally-friendly cycle had a payback period of around 5.5 years and can assist in demand peak shaving of retail buildings. They developed their concept by introducing an efficient cogeneration system with the aim of simultaneous production of power and cooling capacity in peak demand periods [9].

Seawater desalination is an attractive idea for addressing the water supply shortages [18]. Water evaporation and membrane desalination methods are two major methods; reverse osmosis (RO) is the most well-known example of membrane desalination and requires low energy supply [19]. Nevertheless, it has a high maintenance cost and produces water containing remnant bromides and chlorides [20]. Multi-effect desalination (MED), multistage flash (MSF) and multi-effect desalination with thermal vapor compression (MED-TVC) are thermal methods that can use non-potable water with various characteristics such as excessive salinity [21]. Thermally driven systems such as MED and MSF, perhaps combined with RO are pioneering novel desalination technologies [22]. MED remains an excellent selection for large-scale desalination because of advantages such as lower operating temperature, capital cost, and capability for scaling-up, in comparison with MSF for example. In this regard, several researches have been undertaken to examine a combination of MED with various renewable energy and auxiliary systems. Khalilzade et al. [23] investigated a hybrid cycle combining MED and wind turbines, wherein drinkable water is provided by recovering the dissipated heat of the wind turbines in an area with average wind velocity of 11 m/s as the MED heating source. Mokhtari et al. [24] proposed an integrated system containing a gas turbine, MED, and RO for brackish water desalination. Elsayed et al. [25] performed the exergoeconomic evaluation of a MED-TVC system and concluded that the evaporators are responsible for 52% of the overall exergy destruction. Askari et al. [26] investigated a solar rankine cycle (SRC) combined with thermal sources from natural gas and solar linear Fresnel (LF) technology. They used an MED system to produce distilled water by using 70 °C water vapor coming from the SRC turbine outlet. Moradi et al. [27] analyzed a cogeneration system including Stirling engine, fuel cell, and MED units for simultaneous production of water and electricity. Their results showed that appreciable amounts of freshwater can be coproduced using waste heat recovery in the hybrid system. Xue et al. [28] integrated a low-temperature MED system with a coal-fired power plant with the aim of peak shaving and improving its efficiency and power dispatchability. Ghorbani et al. [29] developed and scrutinized a trigeneration system based on MED, an absorption chiller and a molten carbonate fuel cell from the energy and exergy points of view and for the scale of systems they chose, demonstrated they could provide 72 MW electricity, 32 MW cooling capacity and 119 ton/h freshwater, simultaneously.

Water and energy are two inextricably linked and existential resources, and hybridization of CAES and desalination systems can be a promising idea for the simultaneous management of water and energy issues. This combination has not been previously studied. Unlike the PHES, CAES can be used in different geological locations such as dry

and warm environments, where both power and potable water are crucial. A novel integrated configuration of CAES and MED is presented in this research to address both power and water needs. The proposed system is designed to provide drinkable water in both the charging and discharging modes. To this end, heat losses in turbine and compressor exhausts are recovered in the MED unit for producing distilled water during peak and off-peak periods, respectively. The HTES component has been employed instead of conventional combustion chambers in the CAES power output unit to reduce fossil fuel consumption, thereby reducing $CO_2$ emissions, which impact global warming and ozone depletion. Furthermore, a significant *RTE* improvement from waste heat recovery is achieved, comparing favorably with the work of others in different processes (e.g. Razmi et al. [8]). Hence, achieving peak shaving capabilities from CAES with high overall efficiency, low environmental effects and the simultaneous production of pure water appear to be advantageous of this proposed CAES-MED system. Exploring the effect of maximum to minimum pressure ratio of the CAES tank as a significant factor on *RTE*, the volume of the CAES tank and the operating period of the system is another investigation in this study that appear not to has been previously addressed.

## 2. System description

Fig. 1 is a schematic diagram of the CAES-MED system, which includes two main units: compressed air energy storage and multi-effect desalination units.

The CAES unit includes a compression train, a CAES vessel, a pressure regulating valve, a recuperator and a HTES. Two air compressors with identical compression ratios are used to decrease the power consumption of the compression train. During off-peak periods, excess and cheap electricity drives the air compressors and generates heat in HTES via joule-resistance heating. A refractory concrete with implanted electrical cartridge heaters and steel pipes is preferred as the HTES solid material [9]. Since the compression process generates a large amount of heat, an intercooler and aftercooler are used to capture the released heat. To prevent heat dissipation and exergy destruction, the captured heat is directly carried to the desalination unit for producing potable water. So, not only is waste heat recovered, but decreasing the inlet air temperature of the second compressor and the CAES vessel respectively reduces their power consumption and design volume.

During discharge, the air in the CAES vessel is regulated to a constant pressure and then preheated in the recuperator and the HTES before power generation. The HTES component is used instead of conventional combustion chambers to reduce environmental impacts. Finally, the turbine is driven by the hot compressed air and power provided in peak demand periods. Although a subtotal of the high energy density in the air exiting the turbine is taken by the recuperator, it still has high heating value, and the remaining heat is used as the heat source for the MED unit to improve overall system efficiency. Thus, both power and potable water are simultaneously produced in peak power demand periods.

The proposed MED unit consists of 14 stages in which the desalination process in all stages have the same procedure except stages 1 and 14. The main MED components include evaporator, demister, flash chamber, steam mixer and condensate mixer. The entire heat needs for the MED unit are provided at the first stage. Feed water enters the first stage at the saturation temperature (Fig. 2) and after receiving the required heat in the evaporator section, a portion of the water evaporates and the rest accumulates at the bottom to be reused as the feed water for the next stage. The evaporated water passes through the demister section, which filters salt residues from the vapor. In the preheating unit, the vapor is partially condensed to preheat the feed water entering cell 1. The remaining vapor acts as the heat source for the next stage, and the condensed vapor goes into the distilled water reservoirs.

The disposition of the middle stages (stages 2–13) is shown in Fig. 3. The remnant undistilled water of the previous cell is used as the feed water for the next stage. Pressure drops in each stage lead to partial evaporation of the water before feeding to the evaporator section. Finally, the remaining water vapor of the previous stage is condensed in the evaporator section.

In the last stage (Fig. 4), the desalination process streams from all stages are gathered and introduced to the heat exchanger. A higher amount of water is required to condense the water vapor, so extra water

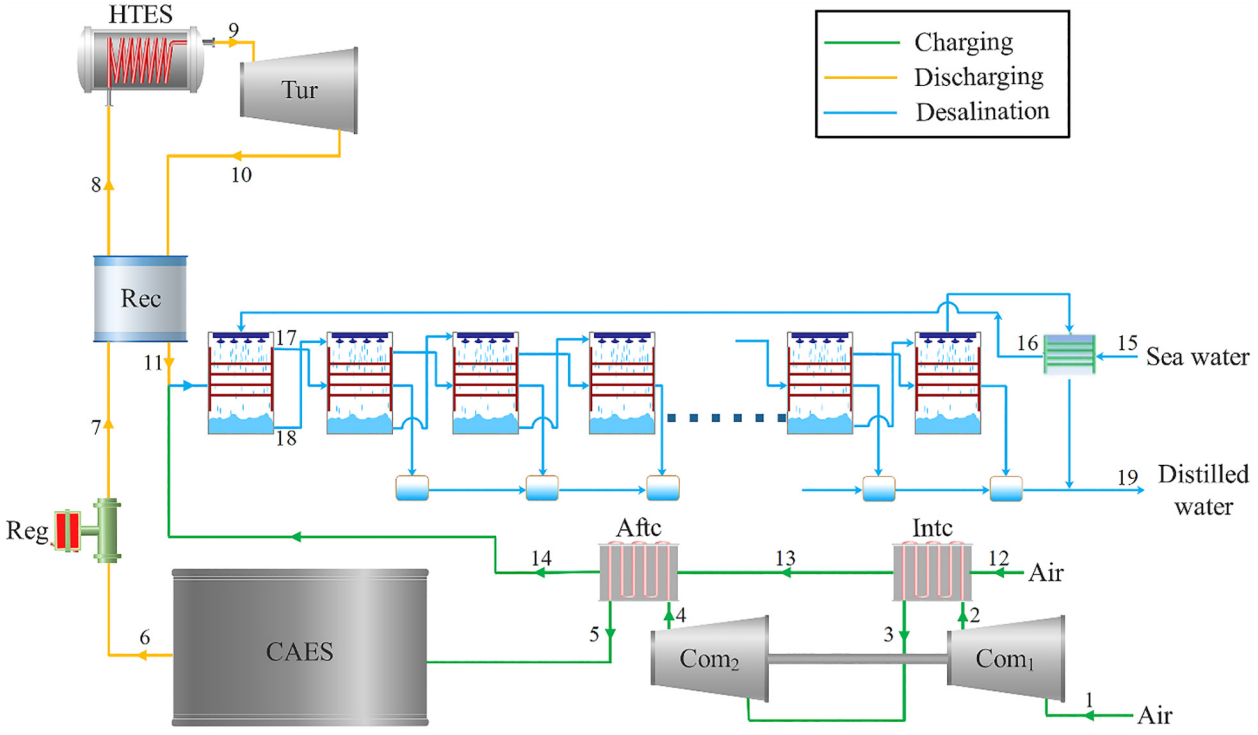


**Fig. 1.** The schematic diagram of the proposed hybrid CAES-MED system.

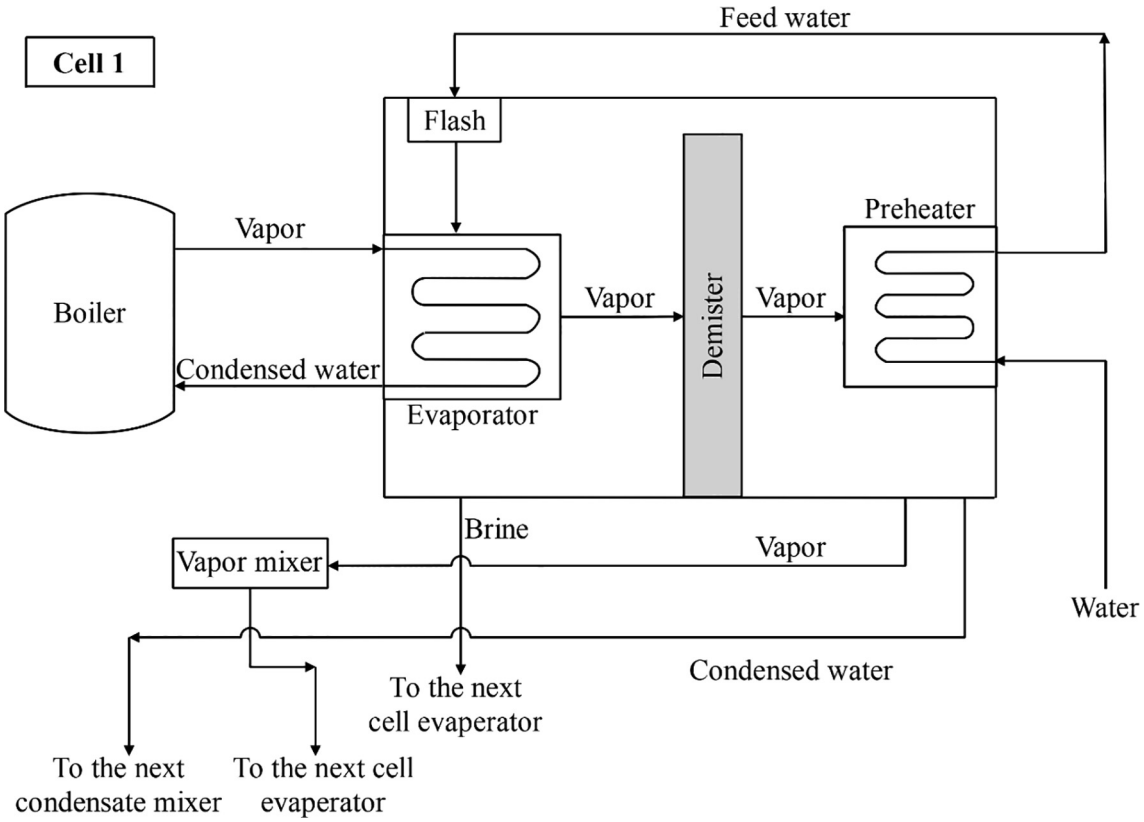


**Fig. 2.** First stage of the desalination unit.

is used in the preheater section of the last stage and then returned to the source (e.g. the sea or the well). Finally, the distilled water stream is produced and the remained non-potable underflow is disposed.

## 3. Mathematic modeling

The following assumptions are made to simplify the analysis of the CAES and MED units of the proposed hybrid system [9]:

(1) Air is considered as an ideal gas;

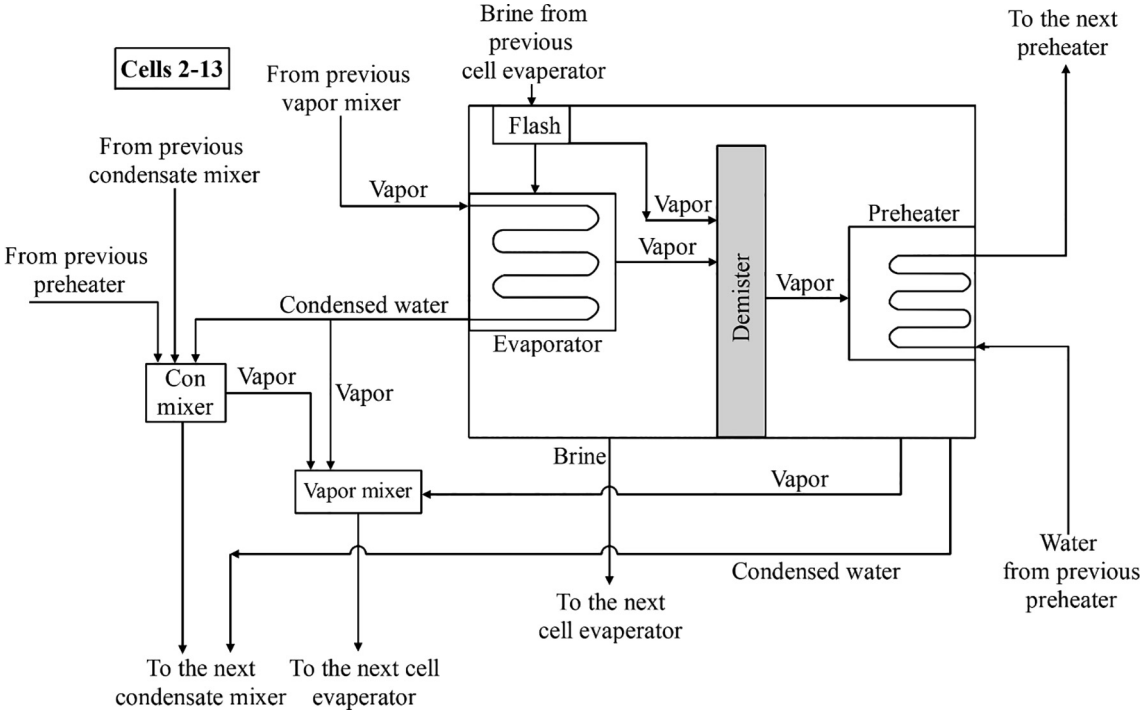


**Fig. 3.** Stages 2–13 of the desalination unit.

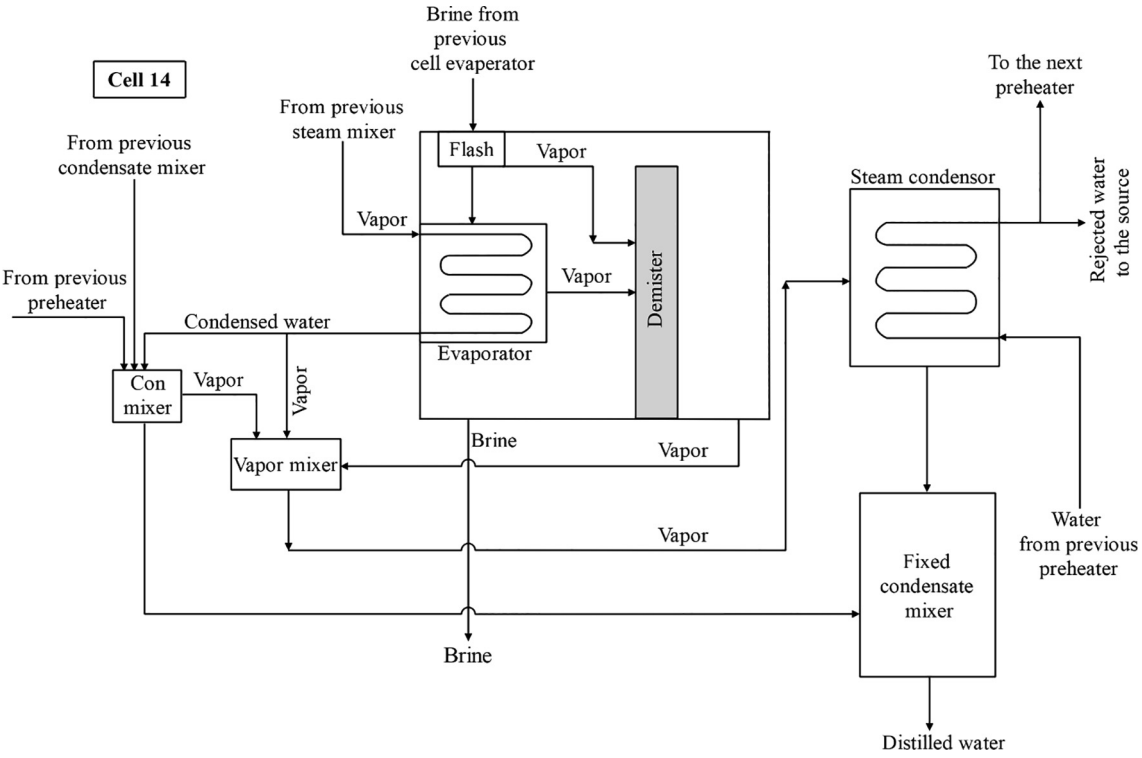


**Fig. 4.** Stage 14 of the desalination unit.

(2) Kinetic and potential energies are ignored;
(3) The isentropic efficiencies of the compressors and turbine are set to be constant;
(4) All of the components operate in steady-state condition;
(5) The charging period is 3 times the discharging period, which leads to a 3 times higher mass flow rate during discharging;
(6) Seawater salinity is constant.

### 3.1. Compressed air energy storage unit

The energy balancing equations for the different components of the proposed CASE unit are expressed here.

#### 3.1.1. Compressors

Cheap excess power is consumed by the compressors during off-peak periods. Two air compressors with identical compression ratios are selected for providing the required pressure of the CAES tank with minimum electricity consumption. The isentropic efficiency of the compressors are defined by [30]:

$$\eta_{com} = \frac{h_{out,s} - h_{in}}{h_{out} - h_{in}} \tag{1}$$

The power consumption of each compressor is obtained by:

$$\dot{W}_{com} = \dot{m}_{in} \frac{C_P\, T_{in}}{\eta_{com}} \left[ (C_{r,com})^{\frac{K-1}{K}} - 1 \right] \tag{2}$$

The overall power consumption of the compression train can be expressed as:

$$\dot{W}_{com} = \dot{W}_{com\,1} + \dot{W}_{com\,2} \tag{3}$$

#### 3.1.2. Heat exchangers

The governing energy balancing equations for the intercooler, aftercooler and MED boiler during charging, and recuperator and MED boiler during discharging are respectively expressed as:

$$\dot{m}_c (h_{13} - h_{12}) = \dot{m}_{in} (h_2 - h_3) \tag{4}$$

$$\dot{m}_c (h_{14} - h_{13}) = \dot{m}_{in} (h_4 - h_5) \tag{5}$$

$$\dot{Q}_{Des,\,ch} = \dot{m}_c (h_{14} - h_{14'}) \tag{6}$$

$$h_8 - h_7 = h_{10} - h_{11} \tag{7}$$

$$\dot{Q}_{Des,\,dsch} = \dot{m}_{out} (h_{11} - h_{11'}) \tag{8}$$

#### 3.1.3. Compressed air storage tank

The operational periods of the hybrid system during peak and off-peak times are a function of their mass flow rates and densities, which can be calculated by [8]:

$$t_{ch} = \frac{(\rho_5 - \rho_7) V_{CAES}}{3600\, \dot{m}_{in}} \tag{9}$$

$$t_{dsch} = \frac{(\rho_5 - \rho_7) V_{CAES}}{3600\, \dot{m}_{out}} \tag{10}$$

#### 3.1.4. Pressure-regulating valve

The compressed air in the CAES tank is released during the peak demand period to run the air turbine. Governing energy balancing equation for the pressure regulating valve is as follows [31]:

$$h_6 = h_7 \tag{11}$$

#### 3.1.5. High temperature thermal energy storage

The required heating energy and mass size of the HTES material for attaining a constant design turbine entry temperature are calculated as follows [8]:

$$\dot{Q}_{HTES} = \dot{m}_{out} (h_9 - h_8) \tag{12}$$

$$M_{HTES} = \frac{\dot{Q}_{HTES} \cdot\, t_{Dch}}{C_{HTES} (T_{\max,\,HTES} - T_{\min,\,HTES})} \tag{13}$$

#### 3.1.6. Turbine

The heated air enters the turbine to generate power during peak demand periods. The isentropic efficiency of the turbine and the generated power are calculated by:

$$\eta_{Tur} = \frac{h_{in} - h_{out}}{h_{in} - h_{out,s}} \tag{14}$$

$$\dot{W}_{Tur} = \dot{m}_{out}.\ C_P.\ \eta_{Tur}.\ T_9\left[1 - \left(\frac{P_{10}}{P_9}\right)^{\frac{K-1}{K}}\right] \tag{15}$$

### 3.2. Multi-effect desalination unit

As explained in Section 2, there are three different configurations for the stages of the MED unit: first stage, middle stages, and the final stage. The mass, salt, and energy balancing equations for all stages are presented in the following subsections:

#### 3.2.1. Mass balancing equations

The mass balancing equations for different stages and their components are indicated in Table 1. Since there are different components in various stages, different equations are needed for simulation of each stage.

#### 3.2.2. Salt mass balancing equations

The salt balancing equations are also different for each MED stage in Table 2. The salt mass concentration and mass flow rate are the two key factors for evaluating the salt mass balancing equations.

#### 3.2.3. Energy balancing equations

Moreover, the governing energy balancing equations for the various stages of the MED unit are specified in Table 3.

The key design values of the proposed hybrid CAES-MED system during the calculation process are listed in Table 4.

### 3.3. Performance assessment

The proposed hybrid CAES-MED system involves two energy inputs to the system during off-peak periods: Power for the compression train and HTES. Power and distilled water are the outputs of the system; power is generated in peak demand periods, whereas distilled water is produced in both the charging and discharging modes. As the charging and discharging times are not identical nor simultaneous, a conventional performance equation derived from the first law of thermodynamics cannot be used. Consequently, the efficiency of the combined CAES-MED system is defined by the round trip efficiency (*RTE*) [8]:

$$RTE = \frac{t_{ch}.\ (\dot{Q}_{Des,\,ch} - \dot{Q}_{Diss,\,ch}) + t_{dsch}.\ (\dot{Q}_{Des,\,dsch} - \dot{Q}_{Diss,\,dsch}) + t_{dsch}.\ \dot{W}_{Tur}}{t_{ch}\,(\dot{W}_{Com} + \dot{W}_{HTES})} \tag{16}$$

Also, the efficiency of the MED unit is calculated by the performance ratio (*PR*) as follows [32]:

$$PR = \frac{\dot{m}_{dis,\,ch} \times 2300}{\dot{Q}_{Des,\,ch}} = \frac{\dot{m}_{dis,\,dsch} \times 2300}{\dot{Q}_{Des,\,dsch}} \tag{17}$$

**Table 2**
Salt mass balancing equations for different stages of desalination unit.

| | |
|---|---|
| First stage | $\dot{m}_{SW_{P1}}.\ X_{SW_{P1}} = \dot{m}_{BR_{F1}}.\ X_{BR_{F1}}$<br>$\dot{m}_{BR_{F1}}.\ X_{BR_{F1}} = \dot{m}_{BR_{E1}}.\ X_{BR_{E1}}$ |
| Middle stages | $\dot{m}_{BR_{E(n-1)}}.\ X_{BR_{E(n-1)}} = \dot{m}_{BR_{F(n)}}.\ X_{BR_{F(n)}}$<br>$\dot{m}_{BR_{F(n)}}.\ X_{BR_{F(n)}} = \dot{m}_{BR_{E(n)}}.\ X_{BR_{E(n)}}$ |
| Final stage | $\dot{m}_{BR_{E13}}.\ X_{BR_{E13}} = \dot{m}_{BR_{F14}}.\ X_{BR_{F14}}$<br>$\dot{m}_{BR_{F14}}.\ X_{BR_{F14}} = \dot{m}_{BR_{E14}}.\ X_{BR_{E14}}$ |

## 4. Validation

Apparently, the proposed hybrid CAES-MED system has not been studied in the literature, so each of the CAES and MED units is individually validated, and the results are shown in Table 5 [8,32]. These results are almost equal to results in related publications with minor differences, therefore, the simulation results are considered to be reliable.

## 5. Results and discussion

In this section, the simulation results of the CAES-MED system are presented based on the design conditions, listed in Table 4.

### 5.1. Thermodynamic analysis

The results of the thermodynamic simulation for the streams of the combined CAES-MED system are indicated in Table 6.

By employing the calculated data of Table 6 in the governing equations presented in section 3, the efficiency results of the hybrid CAES-MED system are calculated and listed in Table 7. As seen, 24051 kW and 30863 kW power are respectively consumed in the compressors and the HTES for compressing the ambient air and storing heat during the off-peak period. During the compression process, 9433 kW and 10875 kW of heat power are recovered by the intercooler and aftercooler, which is directly transferred to the MED unit. However, only 9239 kW of the recovered heat is efficiently recycled by the MED unit, which leads to the production of 38.06 kg/s distilled water in the charging mode for 7.785 hrs. During discharging, 80054 kW electrical energy is generated in 2.595 hrs by the expansion of pressurized air through the turbine. Moreover, 15179 kW of the hot flue gas in the turbine exhaust is recovered by the MED unit after passing through the recuperator. As a result, 62.53 kg/s potable water is produced during discharging. The results indicate that 1638 ton HTES material (refractory concrete) is required for storing 30,863 kW heating power. By

**Table 1**
Mass balancing equations for different stages of desalination unit.

| First stage | Middle stages | Final stage |
|---|---|---|
| $\dot{m}_{SW_{P1}} = \dot{m}_{BR_{F1}}$ | $\dot{m}_{BR_{E(n-1)}} = \dot{m}_{BR_{F(n)}} + \dot{m}_{ST_{F(n)}}$ | $\dot{m}_{BR_{E13}} = \dot{m}_{BR_{F14}} + \dot{m}_{ST_{F14}}$ |
| $\dot{m}_{BR_{F1}} = \dot{m}_{ST_{E1,\,out}} + \dot{m}_{BR_{E1}}$ | $\dot{m}_{BR_{F(n)}} = \dot{m}_{ST_{E(n),\,out}} + \dot{m}_{BR_{E(n)}}$ | $\dot{m}_{BR_{F14}} = \dot{m}_{ST_{E14,\,out}} + \dot{m}_{BR_{E14}}$ |
| $\dot{m}_{ST_{E1,\,out}} = \dot{m}_{ST_{D1}}$ | $\dot{m}_{ST_{M(n-1)}} = \dot{m}_{CO_{E(n)}} + \dot{m}_{ST_{E(n)}}$ | $\dot{m}_{ST_{M13}} = \dot{m}_{CO_{E14}} + \dot{m}_{ST_{E14}}$ |
| $\dot{m}_{ST_{D1}} = \dot{m}_{ST_{P1}} + \dot{m}_{CO_{P1}}$ | $\dot{m}_{ST_{E(n),\,out}} = \dot{m}_{ST_{F(n)}} + \dot{m}_{ST_{D(n)}}$ | $\dot{m}_{ST_{E14,\,out}} = \dot{m}_{ST_{F14}} + \dot{m}_{ST_{D14}}$ |
| $\dot{m}_{SW_{P1}} = \dot{m}_{SW_{P2}}$ | $\dot{m}_{ST_{D(n)}} = \dot{m}_{ST_{P(n)}} + \dot{m}_{CO_{P(n)}}$ | $\dot{m}_{ST_{M14}} = \dot{m}_{CO_{Con}}$ |
| $\dot{m}_{ST_{P1}} = \dot{m}_{ST_{M1}}$ | $\dot{m}_{SW_{P(n+1)}} = \dot{m}_{SW_{P(n)}}$ | $\dot{m}_{SW} = \dot{m}_{SW_{Con}} + \dot{m}_{SW_R}$ |
| | $\dot{m}_{ST_{M(n)}} = \dot{m}_{ST_{P(n)}} + \dot{m}_{ST_{E(n)}} + \dot{m}_{ST_{CM(n)}}$ | $\dot{m}_{ST_{M14}} = \dot{m}_{ST_{E14}} + \dot{m}_{ST_{CM14}} + \dot{m}_{ST_{D14}}$ |
| | $\dot{m}_{CO_{P(n-1)}} + \dot{m}_{CO_{CM(n-1)}} + \dot{m}_{CO_{E(n)}} = \dot{m}_{ST_{CM(n)}} + \dot{m}_{CO_{CM(n)}}$ | $\dot{m}_{CO_{P13}} + \dot{m}_{CO_{CM13}} + \dot{m}_{CO_{E14}} = \dot{m}_{ST_{CM14}} + \dot{m}_{CO_{CM14}}$ |

**Table 3**
Energy balancing equations for various components in different stages of desalination unit.

| | |
|---|---|
| First stage | $\dot{m}_{SW_{P1}}.\ h_{SW_{P1}} = \dot{m}_{BR_{F1}}.\ h_{BR_{F1}}$ |
| | $\dot{Q}_{Des} + \dot{m}_{BR_{F1}}.\ h_{BR_{F1}} = \dot{m}_{ST_{E1,\,out}}.\ h_{ST_{E1,\,out}} + \dot{m}_{BR_{E1}}.\ h_{BR_{E1}}$ |
| | $\dot{m}_{ST_{E1,\,out}}.\ h_{ST_{E1,\,out}} = \dot{m}_{ST_{D1}}.\ h_{ST_{D1}}$ |
| | $\dot{m}_{ST_{D1}}.\ h_{ST_{D1}} + \dot{m}_{SW_{P2}}.\ h_{SW_{P2}} = \dot{m}_{ST_{P1}}.\ h_{ST_{P1}} + \dot{m}_{CO_{P1}}.\ h_{CO_{P1}} + \dot{m}_{SW_{P1}}.\ h_{SW_{P1}}$ |
| | $\dot{m}_{ST_{P1}}.\ h_{ST_{P1}} = \dot{m}_{ST_{M1}}.\ h_{ST_{M1}}$ |
| Middle stages | $\dot{m}_{BR_{E(n-1)}}.\ h_{BR_{E(n-1)}} = \dot{m}_{BR_{F(n)}}.\ h_{BR_{F(n)}} + \dot{m}_{ST_{F(n)}}.\ h_{ST_{F(n)}}$ |
| | $\dot{m}_{BR_{F(n)}}.\ h_{BR_{F(n)}} + \dot{m}_{ST_{M(n-1)}}.\ h_{ST_{M(n-1)}} = \dot{m}_{ST_{E(n),out}}.\ h_{ST_{E(n),out}} + \dot{m}_{BR_{E(n)}}.\ h_{BR_{E(n)}} + \dot{m}_{CO_{E(n)}}.\ h_{CO_{E(n)}} + \dot{m}_{ST_{E(n)}}.\ h_{ST_{E(n)}}$ |
| | $\dot{m}_{ST_{E(n),\,out}}.\ h_{ST_{E(n),\,out}} + \dot{m}_{ST_{F(n)}}.\ h_{ST_{F(n)}} = \dot{m}_{ST_{D(n)}}.\ h_{ST_{D(n)}}$ |
| | $\dot{m}_{ST_{D(n)}}.\ h_{ST_{D(n)}} + \dot{m}_{SW_{P(n+1)}}.\ h_{SW_{P(n+1)}} = \dot{m}_{ST_{P(n)}}.\ h_{ST_{P(n)}} + \dot{m}_{CO_{P(n)}}.\ h_{CO_{P(n)}} + \dot{m}_{SW_{P(n)}}.\ h_{SW_{P(n)}}$ |
| | $\dot{m}_{ST_{P(n)}}.\ h_{ST_{P(n)}} + \dot{m}_{ST_{E(n)}}.\ h_{ST_{E(n)}} + \dot{m}_{ST_{CM(n)}}.\ h_{ST_{CM(n)}} = \dot{m}_{ST_{M(n)}}.\ h_{ST_{M(n)}}$ |
| | $\dot{m}_{CO_{P(n-1)}}.\ h_{CO_{P(n-1)}} + \dot{m}_{CO_{CM(n-1)}}.\ h_{CO_{CM(n-1)}} + \dot{m}_{CO_{E(n)}}.\ h_{CO_{E(n)}} = \dot{m}_{ST_{CM(n)}}.\ h_{ST_{CM(n)}} + \dot{m}_{CO_{CM(n)}}.\ h_{CO_{CM(n)}}$ |
| Final stage | $\dot{m}_{BR_{E13}}.\ h_{BR_{E13}} = \dot{m}_{BR_{F14}}.\ h_{BR_{F14}} + \dot{m}_{ST_{F14}}.\ h_{ST_{F14}}$ |
| | $\dot{m}_{BR_{F14}}.\ h_{BR_{F14}} + \dot{m}_{ST_{M13}}.\ h_{ST_{M13}} = \dot{m}_{ST_{E14,out}}.\ h_{ST_{E14,out}} + \dot{m}_{BR_{E14}}.\ h_{BR_{E14}} + \dot{m}_{CO_{E14}}.\ h_{CO_{E14}} + \dot{m}_{ST_{E14}}.\ h_{ST_{E14}}$ |
| | $\dot{m}_{ST_{E14,\,out}}.\ h_{ST_{E14,\,out}} + \dot{m}_{ST_{F14}}.\ h_{ST_{F14}} = \dot{m}_{ST_{D14}}.\ h_{ST_{D14}}$ |
| | $\dot{m}_{ST_{M14}}.\ h_{ST_{M14}} + \dot{m}_{SW}.\ h_{SW} = \dot{m}_{CO_{Con}}.\ h_{CO_{Con}} + \dot{m}_{SW_{Con}}.\ h_{SW_{Con}} + \dot{m}_{SW_R}.\ h_{SW_R}$ |
| | $\dot{m}_{ST_{E14}}.\ h_{ST_{E14}} + \dot{m}_{ST_{CM14}}.\ h_{ST_{CM14}} + \dot{m}_{ST_{D14}}.\ h_{ST_{D14}} = \dot{m}_{ST_{M14}}.\ h_{ST_{M14}}$ |
| | $\dot{m}_{CO_{P13}}.\ h_{CO_{P13}} + \dot{m}_{CO_{CM13}}.\ h_{CO_{CM13}} + \dot{m}_{CO_{E14}}.\ h_{CO_{E14}} = \dot{m}_{ST_{CM14}}.\ h_{ST_{CM14}} + \dot{m}_{CO_{CM14}}.\ h_{CO_{CM14}}$ |

**Table 4**
Key design values of the hybrid CAES-MED system.

| Parameter | Unit | Value |
|---|---|---|
| Air gas constant | kJ/kg.K | 0.287 |
| Ambient pressure | bar | 1.01 |
| Ambient temperature | °C | 25 |
| CAES vessel volume | $m^3$ | 60,000 |
| Heat exchanger effectiveness | % | 80 |
| Inlet mass flow rate of CAES vessel | kg/s | 50 |
| Inlet temperature of turbine | °C | 900 |
| Intercooler and aftercooler effectiveness | % | 80 |
| Isentropic efficiency of air compressors | % | 88 |
| Isentropic efficiency of turbine | % | 88 |
| Maximum pressure of CAES vessel | bar | 40 |
| Maximum temperature of HTES | °C | 1200 |
| Minimum pressure of CAES vessel | bar | 13.33 |
| Minimum temperature of HTES | °C | 600 |
| Operating temperature of MED unit | °C | 70 |
| Outlet mass flow rate of CAES vessel | kg/s | 150 |
| Pinch temperature | °C | 10 |
| Recovery heated air mass flow rate | kg/s | 200 |
| Recuperator effectiveness | % | 80 |
| Sea water salinity | % | 0.035 |
| Specific heat capacity of HTES | kJ/kg.K | 0.88 |
| Specific heat of air at constant pressure | kJ/kg.K | 1 |
| Specific heat of air at constant volume | kJ/kg.K | 0.718 |
| Stage number of MED unit | – | 14 |

**Table 5**
Validation of the simulation results of the present study with Refs. [8,32].

| Parameter | | Present work | Reference | Error (%) |
|---|---|---|---|---|
| CAES | First compressor temperature (K) | 482.67 | 479.80 | 0.59 |
| | Second compressor temperature (K) | 539.83 | 536.00 | 0.71 |
| | Turbine outlet temperature (K) | 778.41 | 781.90 | 0.45 |
| | Round trip efficiency (%) | 56.24 | 56.71 | 0.83 |
| | Output power (kW) | 528.82 | 533.40 | 0.86 |
| MED | Distilled water rate (kg/s) | 0.8175 | 0.8311 | 1.63 |
| | Brine water salinity | 0.0550 | 0.0559 | 1.61 |
| | Operating pressure of cell 1 (bar) | 0.2870 | 0.2650 | 7.66 |
| | Performance ratio | 9.4012 | 9.5576 | 1.63 |

employing a 14-stage MED unit, the *PR* reaches to 9.476. Also, the *RTE* of the proposed system reaches to 69.95%, a 13.24% *RTE* improvement in comparison with the work of Razmi et al. [8].

### 5.2. Parametric analysis

Parametric analysis is carried out to scrutinize the effects of the critical parameters on the system performance [33]. In this regard, the variables are kept constant for evaluating the alteration of a specific parameter.

Fig. 5 shows the effect of stage number of MED unit on *PR* and the distillation rate of water. The water distillation rate is augmented by increasing the number of stages. As the evaporated water at the last stage still has enough heat power, it can be used as the heat source of a further stage to produce somewhat more distilled water. The *PR* is improved by increasing the distillation rate of water in a constant heat power condition as a result of the stage number increment, but the investment cost of the MED unit increases with the number of stages. Note also that more brine water is distilled during the discharging period because of higher exhaust air temperature in comparison to the charging period.

The effect of the first stage operating temperature of the MED unit on *PR* and desalination input power is shown in Fig. 6. With increasing the operating temperature of the first stage, the provided heat power is decreased for both charging and discharging periods. This is because of the reduction of the temperature discrepancy between the aftercooler in charging mode and the recuperator exhausts in discharging mode with the first stage of MED. The distillation rate of water is augmented with increasing the operating temperature in a constant heat energy case as more inlet water gets the required heat energy for evaporation. As a result, heat energy reduction leads to a decrement of the distillation rate, but the temperature increment compensates a portion of this reduction, and consequently, the *PR* is improved.

Fig. 7 demonstrates the effect of the water salinity on *PR* and the distillation rate of water in the discharging period. Increasing the salinity in the case of constant input power and operating water temperature leads to the production of less distilled water and thus a *PR* reduction. This is because of the fact that the reduction of water salinity results in the raising of the saturation temperature and a change $C_p$, specific heat capacity of water. In this article, low to moderate salinities (0.02–0.2) are studied with saturation temperature increments of about 0.6–0.8 °C, which negligibly changes the $C_p$ of the water.

The effect of the inlet air pressure of the CAES tank on *RTE* and the discharging period is presented in Fig. 8. *RTE* is improved with increasing the inlet pressure; however, the slopes of the curves flatten in higher pressures. Higher inlet pressures for the CAES tank leads to smaller volume tanks or to a need for special materials with high burst

**Table 6**
Thermodynamic simulation results for the streams of the hybrid CAES-MED system.

| State | Fluid | T [°C] | P [bar] | h [kJ/kg] | $\dot{m}$ [kg/s] | State | Fluid | T [°C] | P [bar] | h [kJ/kg] | $\dot{m}$ [kg/s] |
|---|---|---|---|---|---|---|---|---|---|---|---|
| 1 | Air | 25.00 | 1.010 | 298.6 | 50.0 | 13 | Air | 71.89 | 1.010 | 345.7 | 200.0 |
| 2 | Air | 256.3 | 6.356 | 533.8 | 50.0 | 14 | Air | 125.7 | 1.010 | 400.1 | 200.0 |
| 3 | Air | 71.27 | 6.356 | 345.1 | 50.0 | $15_{ch}$ | Water | 42.40 | 1.010 | 167.9 | 102.6 |
| 4 | Air | 335.6 | 40.00 | 616.5 | 50.0 | $15_{dsch}$ | Water | 42.40 | 1.010 | 167.9 | 168.6 |
| 5 | Air | 124.6 | 40.00 | 399.0 | 50.0 | $16_{ch}$ | Water | 44.70 | 1.010 | 177.5 | 102.6 |
| 6 | Air | 124.6 | 40.00 | 399.0 | 150.0 | $16_{dsch}$ | Water | 44.70 | 1.010 | 177.5 | 168.6 |
| 7 | Air | 124.6 | 13.33 | 399.0 | 150.0 | $17_{ch}$ | Water | 70.00 | 0.312 | 2626 | 4.381 |
| 8 | Air | 347.7 | 13.33 | 629.2 | 150.0 | $17_{dsch}$ | Water | 70.00 | 0.312 | 2626 | 7.190 |
| 9 | Air | 900.0 | 13.33 | 1246 | 150.0 | $18_{ch}$ | Water | 70.00 | 0.312 | 293.0 | 98.27 |
| 10 | Air | 400.5 | 1.010 | 685.3 | 150.0 | $18_{dsch}$ | Water | 70.00 | 0.312 | 293.0 | 161.4 |
| 11 | Air | 179.8 | 1.010 | 455.1 | 150.0 | $19_{ch}$ | Water | 48.52 | 1.010 | 203.1 | 38.06 |
| 12 | Air | 25.00 | 1.010 | 298.6 | 200.0 | $19_{dsch}$ | Water | 48.52 | 1.010 | 203.1 | 62.53 |

**Table 7**
Simulation results for the proposed hybrid CAES-MED system.

| Parameter | Process | Unit | Value | Parameter | Process | Unit | Value |
|---|---|---|---|---|---|---|---|
| $\dot{W}_{Com\ 1}$ | Charging | kW | 11,924 | $\dot{Q}_{Des,\ dsch}$ | Discharging | kW | 15,179 |
| $\dot{W}_{Com\ 2}$ | Charging | kW | 12,127 | $\dot{Q}_{diss,\ dsch}$ | Discharging | kW | 2732 |
| $\dot{W}_{Com}$ | Charging | kW | 24,051 | $\dot{Q}_{Rec}$ | Discharging | kW | 34,534 |
| $\dot{W}_{HTES}$ | Charging | kW | 30,863 | $\dot{Q}_{HTES}$ | Discharging | kW | 92,588 |
| $\dot{Q}_{Intc}$ | Charging | kW | 9433 | $\dot{W}_{Tur}$ | Discharging | kW | 80,054 |
| $\dot{Q}_{Aftc}$ | Charging | kW | 10,875 | $\dot{m}_{SW,\ dsch}$ | Discharging | kg/s | 168.6 |
| $t_{ch}$ | Charging | hr | 7.785 | $\dot{m}_{dis,\ dsch}$ | Discharging | kg/s | 62.53 |
| $\dot{Q}_{Des,\ ch}$ | Charging | kW | 9239 | $t_{ch}$ | Discharging | hr | 2.595 |
| $\dot{Q}_{diss,\ ch}$ | Charging | kW | 1663 | $M_{HTES}$ | Total | ton | 1638 |
| $\dot{m}_{SW,\ ch}$ | Charging | kg/s | 102.6 | $RTE$ | Total | % | 69.95 |
| $\dot{m}_{dis,\ ch}$ | Charging | kg/s | 38.06 | $PR$ | Total | – | 9.476 |

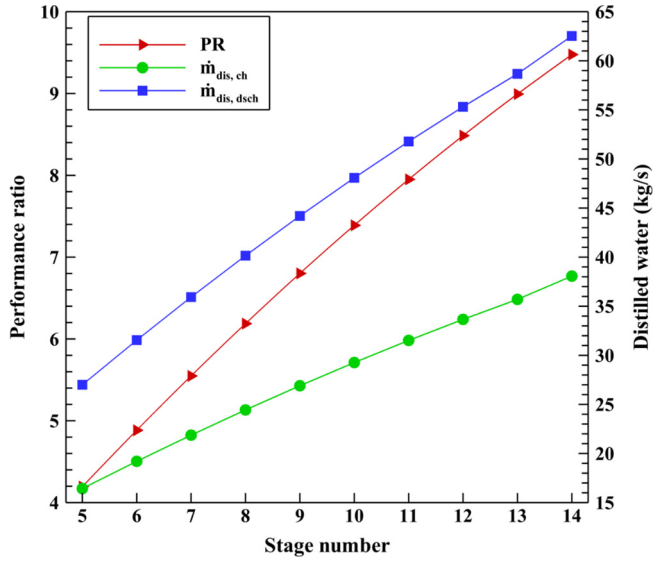


**Fig. 5.** The effect of the stage number on performance ratio and distillation rate of water.

resistance, which increases the capital investment. So, an inlet pressure between 40 and 60 bar is considered more practical for surface vessels, based on vessel materials, economic aspects, and *RTE*. If higher pressures can be obtained at a fixed storage volume for the CAES vessel, more air can be stored at higher pressures and the operating period is linearly increased for a specific CAES volume. In addition, in this study, the impact of the ratio of maximum to minimum (inlet to outlet) pressures on *RTE* and operating period is investigated. The *RTE* is improved in lower pressure ratios; however, the operating period of the system is reduced based on Eqs. ((9) and (10)). Hence, the effect of

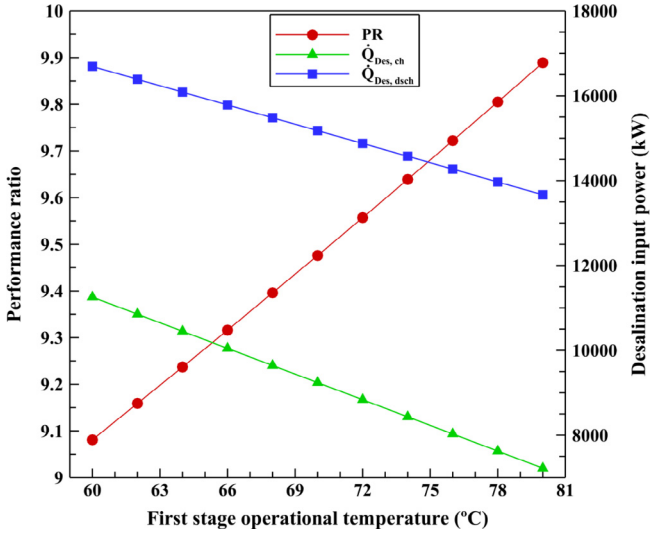


**Fig. 6.** The effect of the first stage operating temperature on performance ratio and desalination input power.

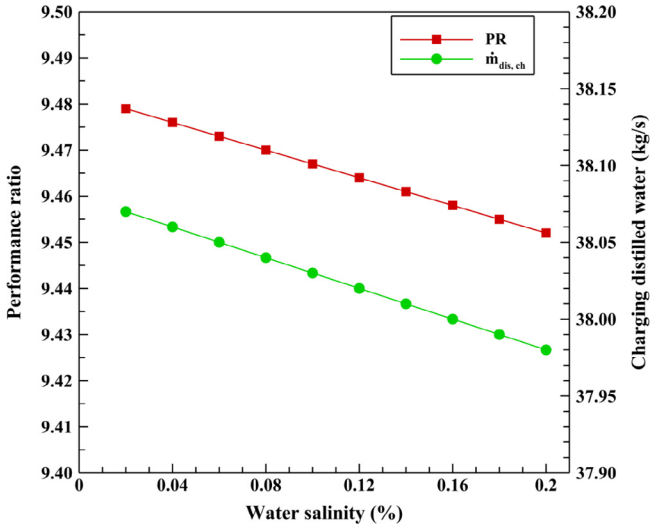


**Fig. 7.** The effect of the water salinity on performance ratio and distillation rate of water.

pressure ratio as a critical parameter for the operating period should be considered and a reasonable ratio based on the desired conditions must be sought.

Fig. 9 represents the impact of the inlet pressure of the CAES tank on distillation rate of water and charging and discharging times based on

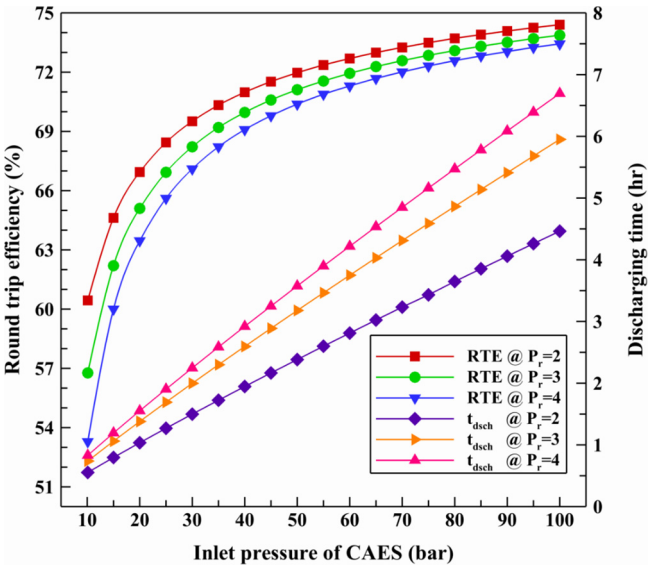


**Fig. 8.** The effect of the inlet pressure of the CAES tank on round trip efficiency and discharging time.

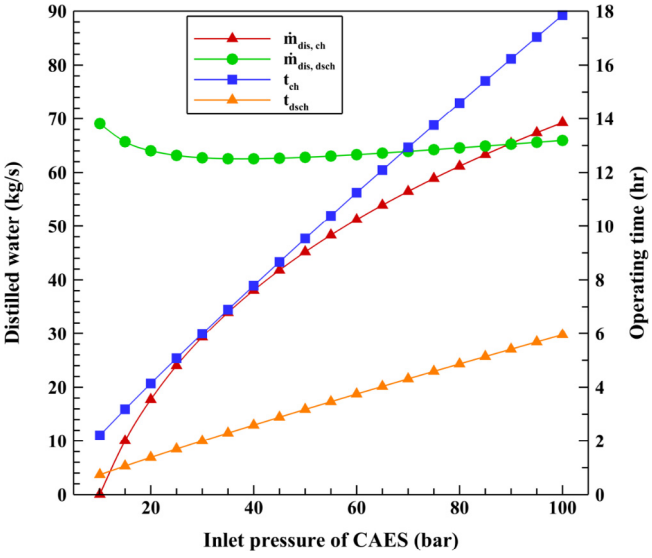


**Fig. 9.** The effect of the inlet pressure of CAES on the distillation rate of water and operating period of the hybrid system.

the design condition. With increasing the inlet pressure of the CAES vessel, the compression ratio of compressors and correspondingly their produced heat augmented. Hence, the recovered heat in intercooler and aftercooler is amplified, which results in higher input heat power of the MED unit and distillation rate of water. Increasing the CAES pressure raises the inlet temperature of the vessel and consequently its outlet temperature in the discharging period ($T_7$). On the other hand, higher pressure for the CAES vessel increases the turbine expansion ratio which decreases the exhaust temperature of the turbine ($T_{10}$). Inlet temperature and input power of MED unit are directly related to the recuperator inlet temperatures ($T_7$ and $T_{10}$). Hence, the distillation rate of water is decreased at the beginning and then improved due to the nonlinear variation of the temperatures with the pressure. Furthermore, both charging and discharging times are extended at higher pressures.

The alteration of the *RTE* and distillation rate of water with respect to the turbine inlet temperature is shown in Fig. 10. Since the MED unit is located downstream of the turbine, any alterations in its working temperature affects produced the distilled water of MED unit. Increasing the inlet temperature of the turbine and consequently, its outlet temperature leads to transferring of much higher input heat power associates to MED unit and consequently producing distilled water with a higher rate. Higher operating temperature for the MED unit leads to a reduction of the temperature discrepancy between its inlet and operating temperatures. The lower temperature gradient means less input heat energy and subsequently lower distilled water production. Thus, the *RTE* of the system is reduced with increasing the operating temperature of the MED unit.

Fig. 11 shows how the inlet mass flow rate of the CAES vessel affects the input heat power to the desalination unit and the distillation rates of the water in both the charging and discharging periods. More heating power is used in the MED unit at higher air mass flow rates (Eqs. ((6) and (8))). Increasing the inlet mass flow rate of the CAES vessel directly affects the discharging mass flow rate, whereas it does not linearly affect the recovered heat at the intercooler and aftercooler in the charging process. Therefore, the slope of distilled water production during discharging is steeper than during charging. A higher inlet heating mass flow rate at the MED unit leads to higher input heating power and therefore larger distilled water production. Thus, the discharging curve of the input heat power and distilled water is steeper than the charging (Fig. 11).

Fig. 12 shows the effect of the operating temperature of the MED unit on the *RTE* and the ratio of distilled water to the total inlet water amount in the MED stages. The MED unit gets the heat only in the first stage, and the produced steam in each previous stage is used as the heat source for the next stage, and the input water in each stage is the warm brine from the previous stage. In successive stages, more distilled water is produced by using a constant heat energy input rate in stage one. The distillation rate of water is reduced in subsequent stages because of the reduction in the water heat content and feed rate. So, the ratio of distilled water amount to the total inlet water is increasing, but with a flatting slope. Since the *RTE* is a function of the electrical energy generated from the turbine, the electrical energy consumed in the compressors and HTES, and also the distilled water in the MED unit, it is improved with higher stage numbers as a result of distilled water production enhancement (but at higher capital cost). Fig. 12 shows that *RTE* declines with a higher operating temperature. This is because of the reduction of the temperature discrepancy between the outlet temperature of the CAES flues and the operating temperature, which reduces the input heat power of the MED unit. The ratio of distilled water amount to the total input water in the MED unit is increased at higher

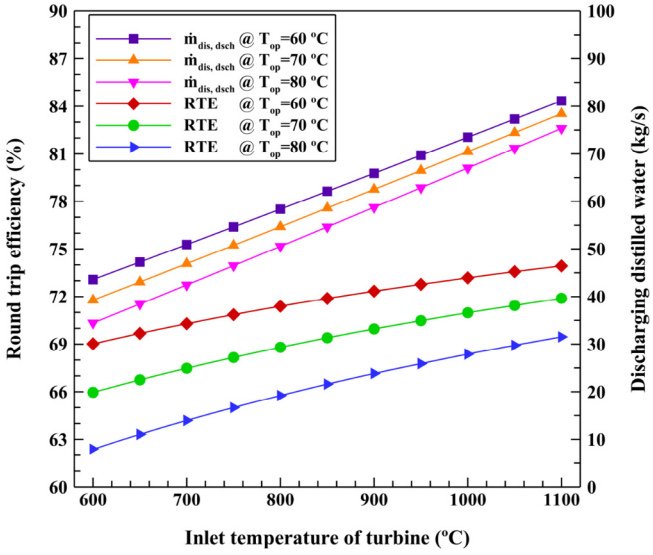


**Fig. 10.** The effect of the inlet temperature of turbine on round trip efficiency and distillation rate of water during discharging.

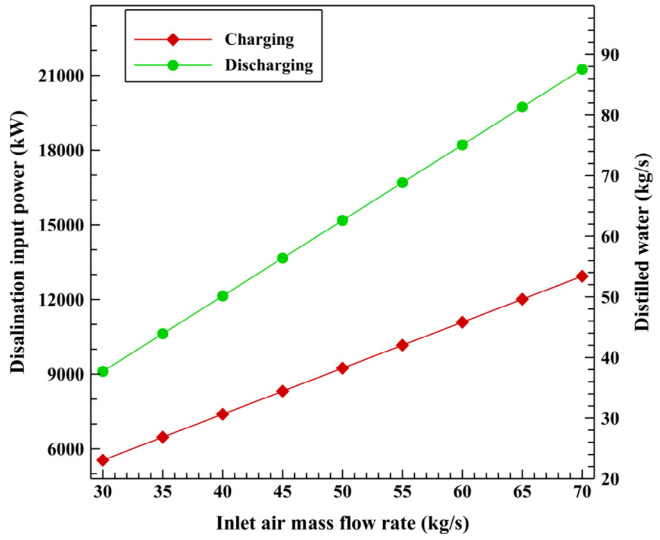


**Fig. 11.** The effect of inlet mass flow rate on desalination input heat power and distillation rate of water.

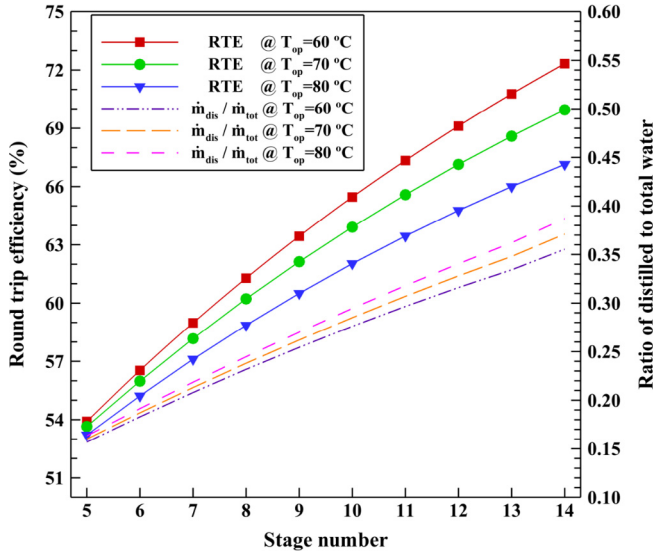


**Fig. 12.** The effect of the stage number on round trip efficiency and the ratio of distilled to total water.

operating temperatures, because only the feed water rate of the first stage is a function of the heat source power and the ratio of distilled water to the total input water amount is independent of heat source power.

Fig. 13 represents the effect of the saline water temperature on the distillation rate of water and brine water salinity. Water temperature is increased in each stage by taking a fraction of the produced steam energy in the preheater, so increasing the heat transfer rate leads to augmentation of the water temperature and reduction of the steam energy which is used in the evaporator of the next stage. In Fig. 13, the distillation rate of water is shown at a constant operating temperature and input heat source power. Increasing the water temperature leads to lower heat exchange in each stage and steam holds much of the energy as the heat power source for the next desalination stage, so more distilled water is produced and the expelled brine is more saline. Thus, since alteration of the operating temperature affects the input heat power, higher operating temperature leads to a lower input heat power, distilled water production rate, and brine water salinity.

## 6. Concluding remarks and future works

In the present article, a novel integrated CAES-MED system was presented and analyzed. The generated heat from the air compression process and turbine exhaust of the CAES unit are recovered by using a MED unit. In contrast to pumped hydro storage (the other feasible grid-scale energy storage technology), a CAES system can be used in different geological surroundings and particularly in dry and hot regions, where providing both potable water and electricity are indispensable. Therefore, combining the processes not only leads to significant improvement of the *RTE*, but also provides simultaneous production of electricity and water to meet the community needs. Parametric scrutiny of the hybrid CAES-MED system was conducted to analyze the influence of various significant parameters on the *RTE*, *PR* and the distillation rate of water. The major conclusions for the hybrid CAES-MED system are summarized:

(1) For the design case analyzed, 38 kg/s distilled water can be generated during the charging period, and 62.5 kg/s distilled water and 80 MW electricity simultaneously provided during the peak demand periods. Modifying the CAES system via adding desalination unit led to a 13.24% *RTE* improvement in comparison to the work of Razmi et al. [8]; the *RTE* of the new hybrid CAES-MED system reaches to about 70%. Furthermore, the *PR* of the MED unit reached about 9.5.

(2) Parametric analysis indicated that the inlet pressure of the CAES vessel between 40 and 60 bar is the most reasonable range based on the type of the CAES vessel material, economic aspects and *RTE* (the variation of *RTE* is ~3% at higher pressures).

(3) Finally, the effect of the maximum to minimum pressure ratio of the CAES tank as a significant factor on *RTE* and operating period of system was explored. In most of the literature, the lower rate of pressure ratio for CAES vessel is taken as a design condition, which leads to *RTE* improvement. However, its negative effect on the CAES vessel volume and the reduction of the system operational time with the aim of peak shaving were neglected.

The novel combination of CAES with desalination systems is promising for the simultaneous production of electricity and potable water, particularly in hot dry climates. The present work revealed a first step towards developing such a hybridization. More work is needed to improve this combination and develop the idea into practice. For example, the combination of CAES with other desalination technologies such as

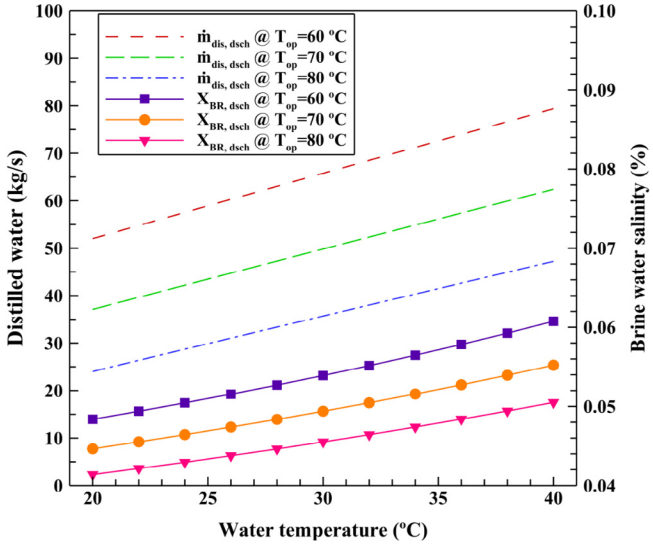


**Fig. 13.** Effect of the water temperature on the distillation rate of water and brine water salinity.

reverse osmosis and also hybridization of liquid air energy storage (LAES) and desalination systems can reduce the volume of the pressurized air tank. The use of multiple steel-cased vertical boreholes in an array can also provide much more flexibility in addressing CAES storage volume and pressure issues [34]. In dry hot climates, the addition of solar thermal energy (rather than photovoltaics) represents an opportunity for further investigation.

## Declaration of Competing Interest

The authors declare that they have no known competing financial interests or personal relationships that could have appeared to influence the work reported in this paper.

## References


[1] Najafi A, Jafarian A, Darand J. Thermo-economic evaluation of a hybrid solar-conventional energy supply in a zero liquid discharge wastewater treatment plant. Energy Convers Manage 2019;188:276–95.

[2] Elia P, Jige S, Ignacio F, Lundblad A, Zhang Y, Ma T, et al. Optimization of a residential district with special consideration on energy and water reliability. Appl Energy 2016;194:751–64.

[3] Khan Z, Linares P, García-gonzález J. Integrating water and energy models for policy driven applications. A review of contemporary work and recommendations for future developments. Renew Sustain Energy Rev 2017;67:1123–38.

[4] Sadeghi S, Askari IB. Prefeasibility techno-economic assessment of a hybrid power plant with photovoltaic, fuel cell and compressed air energy storage (CAES). Energy 2019;168:409–24.

[5] Razmi A, Soltani MA, Kashkooli F, Garousi Farshi L. Energy and exergy analysis of an environmentally-friendly hybrid absorption/recompression refrigeration system. Energy Convers Manage 2018;164:59–69.

[6] Xiaosong Hu, Yuan Hao, Zou Changfu, Zhe Li LZ. Co-estimation of state of charge and state of health for lithium-ion batteries based on fractional-order Calculus. IEEE Trans Veh Technol 2018;67:10319–29.

[7] Hu Xiaosong, Eben Shengbo, Li YY. Advanced machine learning approach for lithium-ion battery state estimation in electric vehicles. IEEE Trans Transp Electrif 2016;2:140–9.

[8] Razmi A, Soltani M, Aghanaja C, Torabi M. Thermodynamic and economic investigation of a novel integration of the absorption-recompression refrigeration system with compressed air energy storage (CAES). Energy Convers Manage 2019;187:262–73.

[9] Razmi A, Soltani M, Torabi M. Investigation of an efficient and environmentally-friendly CCHP system based on CAES, ORC and compression-absorption refrigeration cycle: energy and exergy analysis. Energy Convers Manage 2019;195:1199–211.

[10] Haas J, Cebulla F, Nowak W, Rahmann C, Palma-behnke R. A multi-service approach for planning the optimal mix of energy storage technologies in a fully-renewable power supply. Energy Convers Manage 2018;178:355–68.

[11] Tola V, Meloni V, Spadaccini F, Cau G. Performance assessment of adiabatic compressed air energy storage (A-CAES) power plants integrated with packed-bed thermocline storage systems. Energy Convers Manage 2017;151:343–56.

[12] Chen L, Hu P, Sheng C, Xie M. A Novel compressed air energy storage (CAES) system combined with pre-cooler and using low grade waste heat as heat source. Energy 2017;131:259–66.

[13] He W, Wang J. Optimal selection of air expansion machine in compressed air energy storage: a review. Renew Sustain Energy Rev 2018;87:77–95.

[14] He Q, Liu H, Hao Y, Liu Y, Liu W. Thermodynamic analysis of a novel supercritical compressed carbon dioxide energy storage system through advanced exergy analysis. Renew Energy 2018;127:835–49.

[15] Sadreddini A, Fani M, Ashjari Aghdam M, Mohammadi A. Exergy analysis and optimization of a CCHP system composed of compressed air energy storage system and ORC cycle. Energy Convers Manage 2018;157:111–22.

[16] Zhao P, Wang J, Dai Y. Thermodynamic analysis of an integrated energy system based on compressed air energy storage (CAES) system and Kalina cycle. Energy Convers Manage 2015;98:161–72.

[17] Jannelli E, Minutillo M, Lubrano Lavadera A, Falcucci G. A small-scale CAES (compressed air energy storage) system for stand-alone renewable energy power plant for a radio base station: a sizing-design methodology. Energy 2014;78:313–22.

[18] Moghimi M, Emadi M, Akbarpoor AM, Mollaei M. Energy and exergy investigation of a combined cooling, heating, power generation, and seawater desalination system. Appl Therm Eng 2018;140:814–27.

[19] Behzadi A, Habibollahzade A, Zare V, Ashjaee M. Multi-objective optimization of a hybrid biomass-based SOFC/GT/ double effect absorption chiller/RO desalination system with $CO_2$ recycle. Energy Convers Manage 2019;181:302–18.

[20] Taylor P, Thu K, Kim Y, Myat A, Chakraborty A, Ng KC. Desalination and water treatment performance investigation of advanced adsorption desalination cycle with condenser – evaporator heat recovery scheme. 2012. p. 37–41.

[21] Wakil M, Choon K, Thu K, Baran B. Multi effect desalination and adsorption desalination (MEDAD): a hybrid desalination method. Appl Therm Eng 2014;72:289–97.

[22] Sadri S, Khoshkhoo RH, Ameri M. Optimum exergoeconomic modelling of novel hybrid desalination system (MEDAD + RO). Energy 2018;149:74–83.

[23] Khalilzadeh S, Hossein Nezhad A. Utilization of waste heat of a high-capacity wind turbine in multi effect distillation desalination: energy, exergy and thermoeconomic analysis. Desalination 2018;439:119–37.

[24] Mokhtari H, Sepahvand M, Fasihfar A. Thermoeconomic and exergy analysis in using hybrid systems (GT + MED + RO) for desalination of brackish water in Persian Gulf. Desalination 2016;399:1–15.

[25] Elsayed ML, Mesalhy O, Mohammed RH, Chow LC. Transient and thermo-economic analysis of MED-MVC desalination process. Energy 2019;167:283–96.

[26] Askari IB, Ameri M. Solar rankine cycle (SRC) powered by linear fresnel solar field and integrated with multi effect desalination (MED) system. Renew Energy 2018;117:52–70.

[27] Moradi M, Ghorbani B, Shirmohammadi R, Mehrpooya M, Hamedi M. Developing of an integrated hybrid power generation system combined with a multi-effect desalination unit. Sustain Energy Technol Assess 2019;32:71–82.

[28] Xue Y, Ge Z, Yang L, Du X. Peak shaving performance of coal-fired power generating unit integrated with multi-effect distillation seawater desalination. Appl Energy 2019;250:175–84.

[29] Ghorbani B, Mehrpooya M, Ali S. Hybrid molten carbonate fuel cell power plant and multiple-effect desalination system. J Clean Prod 2019;220:1039–51.

[30] Wang X, Yang C, Huang M, Ma X. Multi-objective optimization of a gas turbine-based CCHP combined with solar and compressed air energy storage system. Energy Convers Manage 2018;164:93–101.

[31] Jiang R, Yin H, Chen B, Xu Y, Yang M, Yang X. Multi-objective assessment, optimization and application of a grid-connected combined cooling, heating and power system with compressed air energy storage and hybrid refrigeration. Energy Convers Manage 2018;174:453–64.

[32] Hatzikioseyian A, Vidali R, Kousi P. Modeling and thermodynamic analysis of a multi effect distillation (MED) plant for sea water desalination. Improving of human potential (IHP) research results at plataforma solar de Almeria, Spain. 2003. p. 17–25.

[33] Kholghi SA, Mahmoudi SMS. Energy and exergy analysis of a modified absorption cycle: A comparative study. Sustain Energy Technol Assessments 2019;32:19–28.

[34] https://cleantechgeo.com/.